IET Communications

Research Article

IET Journals
The Institution of Engineering and Technology

Quadrature spatial modulation based multiuser MIMO transmission system

ISSN 1751-8628
Received on 30th May 2019
Revised 31st October 2019
Accepted on 29th January 2020
E-First on 19th March 2020
doi: 10.1049/iet-com.2019.0573
www.ietdl.org

Francisco Ruben Castillo-Soria[1] ✉, Ertugrul Basar[2], Joaquín Cortez[3], Marco Cardenas-Juarez[1]

[1]*Faculty of Science, Autonomous University of San Luis Potosi, S.L.P., Av Chapultepec 1570. Priv. del Pedregal C.P. 78295, Mexico*
[2]*Communications Research and Innovation Laboratory (CoreLab), Department of Electrical and Electronics Engineering, Koc University, Sariyer 34550, Istanbul, Turkey*
[3]*Department of Electronics and Electrical Engineering, Technological Institute of Sonora, Antonio Caso S/N, Ciudad Obregn, C.P. 85134, Mexico*
✉ *E-mail: ruben.soria@uaslp.mx*

Abstract: This study presents a multiuser (MU) multiple-input multiple-output (MIMO) downlink transmission scheme based on the quadrature spatial modulation (QSM) concept, which uses the indices of the non-zero entries in its transmission vector to modulate and transmit an independent sequence of bits for each user in the system. The MU interference is removed by using a matrix precoding technique based on channel state information (CSI) known as block diagonalisation (BD). The performance of the proposed scheme is compared with the conventional MU–MIMO–BD system for uncorrelated Rayleigh fading channels and correlated fading channels with imperfect CSI in the reception. Additionally, a low-complexity near maximum likelihood (ML) detection algorithm for the MU–MIMO–QSM signal's detection is proposed. For the considered cases, the proposed MU–MIMO–QSM scheme exhibits gains up to 1 dB in bit error rate performance and a reduction in detection complexity up to 93% as compared to the conventional MU–MIMO–BD scheme for the optimal ML detection. The proposed algorithm performs very near to the optimal ML detector whilst achieving a complexity reduction of up to 58%.

1 Introduction

Recently, multiple-input multiple-output (MIMO) and massive MIMO [1] have been recognised as key technologies for the implementation of future wireless communication networks [2]. In a conventional MIMO system, the spatial dimension is used for diversity and/or multiplexing purposes. Nevertheless, recent research has shown the advantages of using the spatial dimension to modulate the transmitted signal [3, 4]. In spatial modulation (SM), the array of transmitting (Tx) antennas is considered as a spatial constellation, where each Tx antenna represents a point in this constellation. Ideally, from each Tx antenna to each receive (Rx) antenna, there exists a different channel that identifies this path. Therefore, by assuming that the wireless channel changes slowly and that the channel state information (CSI) is known, the receiver can determine which Tx antenna has been activated at any given time [5]. In this way, additional information to the transmitted quadrature amplitude modulation (QAM) symbol is transmitted by the active Tx antenna. In particular, quadrature SM (QSM) is an SM-based technique that has the advantage of doubling the number of bits that can be transmitted in the spatial constellation. QSM takes advantage of Tx independently the in-phase and quadrature components of a QAM signal, which results in an improved spectral efficiency (SE) compared to the basic SM scheme [6]. A couple of improvements to this transmission scheme have been proposed in [7, 8]. These previous research findings have motivated novel investigations to study the performance of SM/QSM transmission schemes on multiuser (MU)–MIMO scenarios. In [9], a generalised SM (GSM) MU–MIMO scheme was proposed for the uplink channel and it is shown that the MU–MIMO–GSM scheme outperforms MU–MIMO–SM and conventional MU–MIMO systems. In [10], a precoding matrix is used to transmit an MU–SM signal in the downlink transmission. In this case, the total number of Tx antennas is divided into N_u blocks, which are independently modulated for each user by using only one Rx antenna per user. It is shown that the precoding matrix is an effective way to avoid MU interference.

A block diagonalisation (BD)-based MU–MIMO transmission system [11] that uses SM to transmit additional broadcast information over the conventional MU–MIMO scheme was proposed in [12]. Results show that a number of broadcast transmission bits can be added to the conventional MU–MIMO scheme without performance impairment, at the cost of a slightly increased complexity. In [13], an MU–MIMO scheme that uses space shift keying (SSK) and orthogonal Walsh codes to transmit an MU–MIMO downlink signal is studied. The proposed MU–SSK scheme has reduced detection complexity. However, the throughput is affected by the expansion codes. In [14, 15], the concept of SM at the receiver side is proposed for MU–MIMO systems implementation. In [16], a design criterion of the channel control parameter is provided to reduce the high correlation among different channel coefficients in the hybrid massive MIMO system. In addition, the optimum analogue beamforming vectors are designed with the goal of maximising the signal to leakage and noise ratio in the MU scenario. In [17], a QSM-based non-orthogonal multiple access (NOMA) for MU scenarios was proposed. The main idea of NOMA–QSM is to superimpose several constellation symbols to be transmitted simultaneously via some selected antenna indexes by distinguishing the power domain. As a result, antenna indexes and constellation symbols are perceived at each receiver, improving the SE of the system.

Against this background, in this study, a novel MU–MIMO–QSM downlink transmission scheme for MIMO channels is proposed. The proposed scheme uses the QSM concept to generate an independent transmission vector for each user in the system. Next, a precoding matrix is used in order to cancel the MU interference. All generated signals are combined and transmitted through a wireless channel using the complete Tx antenna array. Additionally, a low-complexity near maximum likelihood (ML) algorithm for the detection of MU–MIMO–QSM signals has been proposed. The contribution of the study is three-fold.

(a) A system which combines BD with QSM techniques to transmit in a MU–MIMO downlink scenario is proposed for two study cases over three different channel conditions.

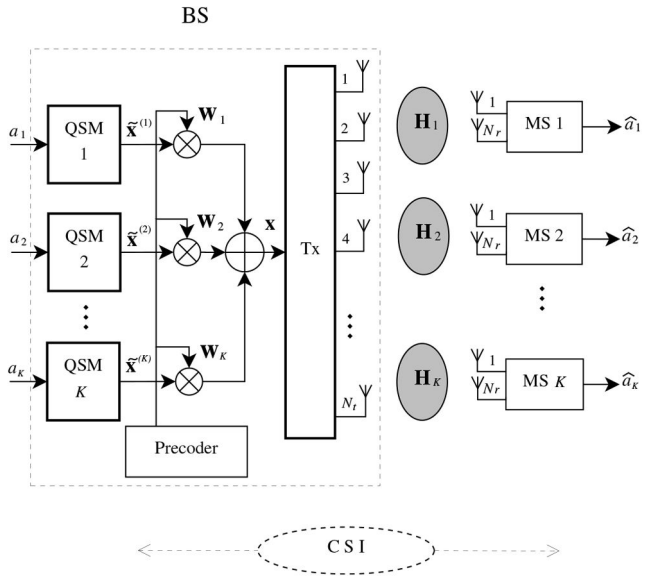

Fig. 1 *MU–MIMO–QSM system model*

Table 1 Example of QSM mapping rule with $L = 2$

Input a	QAM symbol s	Position $(l_{s_\Re}, l_{s_\Im})$	Output vector $\tilde{\boldsymbol{x}}^{(k)}$
0000	$1+j$	(1, 1)	$1+j, 0$
0001	$1+j$	(1, 2)	$1, +j$
0010	$1+j$	(2, 1)	$j, +1$
0011	$1+j$	(2, 2)	$0, 1+j$
0100	$-1+j$	(1, 1)	$-1+j, 0$
0101	$-1+j$	(1, 2)	$-1, +j$
0110	$-1+j$	(2, 1)	$j, -1$
0111	$-1+j$	(2, 2)	$0, -1+j$
1000	$-1-j$	(1, 1)	$-1-j, 0$
1001	$-1-j$	(1, 2)	$-1, -j$
1010	$-1-j$	(2, 1)	$-j, -1$
1011	$-1-j$	(2, 2)	$0, -1-j$
1100	$1-j$	(1, 1)	$1-j, 0$
1101	$1-j$	(1, 2)	$1, -j$
1110	$1-j$	(2, 1)	$-j, +1$
1111	$1-j$	(2, 2)	$0, 1-j$

(b) A novel low complexity near-ML detection algorithm for the MU–MIMO–QSM scheme is proposed.
(c) In order to show the flexibility of the MU–MIMO–QSM scheme, the system is configured for a transmission with a different number of bits per channel use (bpcu) per user and a reduced number of receive antennas.

The proposed scheme is compared with the conventional MU–MIMO–BD system [18] in terms of bit error rate (BER) performance and detection complexity considering the same SE and the same number of Tx and Rx antennas for three different channel scenarios. Results show that the proposed scheme has a BER performance gain of 1 dB and a lower detection complexity up to 93% compared to the conventional MU–MIMO–BD transmission scheme. The proposed low-complexity algorithm performs very near to the optimal ML detector whilst achieving a complexity reduction of up to 58%.

The remainder of this work is organised as follows. In Section 2, the general system model of the MU–MIMO–QSM scheme and a transmission example are introduced. In Section 3, a novel near ML low complexity algorithm for the MU–MIMO–QSM signal's detection is proposed. In Section 4, the results of computer simulations and complexity analysis are offered. Also, the applicability of the proposed system for a reduced number of Tx/Rx antennas is shown. In Section 5, we conclude the work.

Notation: uppercase boldface letters denote matrices whereas lowercase boldface letters denote vectors. The transpose, Hermitian transpose, complex conjugate and Frobenius norm of $\boldsymbol{A}$ are denoted by $\boldsymbol{A}^{\mathrm{T}}$, $\boldsymbol{A}^{\mathrm{H}}$, $\boldsymbol{A}^{*}$, and $\| \boldsymbol{A} \|_{\mathrm{F}}$, respectively. The statistical expectation is represented by $E[\cdot]$. Finally, $\mathscr{CN}(0, \sigma^2)$ is used to represent the circularly symmetric complex Gaussian distribution with variance σ^2.

2 MU–MIMO–QSM transmission system

The system model of the proposed MU–MIMO–QSM downlink transmission scheme is presented in Fig. 1. We consider a base station (BS) with N_{t} transmit antennas and K independent mobile stations or users, each one with N_{r} receiving antennas. Thus, the end-to-end configuration can be considered as a $(K \cdot N_{\mathrm{r}}) \times N_{\mathrm{t}}$ downlink MU–MIMO transmission system. Hence, the system considered here can transmit $m = \log_2(M) + 2\log_2(L)$ bits in each time slot for each user, where M is the size of the M-ary QAM constellation $\mathcal{S} = \{s_1, s_2, \ldots, s_M\}$ and L is the size of the QSM transmission vector for each user. Thus, the general MU MIMO transmission/reception system is mathematically modelled as

$$\begin{bmatrix} y_{k_1} \\ \vdots \\ y_{k_{N_{\mathrm{r}}}} \end{bmatrix} = \sqrt{\gamma} \begin{bmatrix} h_{1,1} & \cdots & h_{1,N_{\mathrm{t}}} \\ \vdots & \ddots & \vdots \\ h_{N_{\mathrm{r}},1} & \cdots & h_{N_{\mathrm{r}},N_{\mathrm{t}}} \end{bmatrix} \begin{bmatrix} x_1 \\ \vdots \\ x_{N_{\mathrm{t}}} \end{bmatrix} + \begin{bmatrix} n_1 \\ \vdots \\ n_{N_{\mathrm{r}}} \end{bmatrix}, \tag{1}$$

which can be expressed equivalently in vector form as

$$\boldsymbol{y}_k = \sqrt{\gamma} \boldsymbol{H}_k \boldsymbol{x} + \boldsymbol{n}_k, \tag{2}$$

where $\boldsymbol{x} \in \mathbb{C}^{N_{\mathrm{t}} \times 1}$ is the overall transmission vector and $\boldsymbol{y}_k \in \mathbb{C}^{N_{\mathrm{r}} \times 1}$ is the received signals' vector of the kth user. $\boldsymbol{H}_k \in \mathbb{C}^{N_{\mathrm{r}} \times N_{\mathrm{t}}}$ is the channel matrix between the BS and the kth user, γ is the signal-to-noise ratio (SNR) at each receiver of each user and $\boldsymbol{n}_k \in \mathbb{C}^{N_{\mathrm{r}} \times 1}$ is the noise vector at the kth user. The noise samples are assumed to be independent and identically distributed (i.i.d.) with $\mathscr{CN}(0, 1)$.

2.1 Quadrature spatial modulation (QSM)

The transmitter is composed by K QSM blocks. Each QSM block is intended for a different user in the system. For the kth user, a sequence of $a_k = \{b_n\}_{n=1}^{m}$ input bits, is fed into kth block. The output vector $\tilde{\boldsymbol{x}}^{(k)} \in \mathbb{C}^{L \times 1}$, is represented by

$$\tilde{\boldsymbol{x}}^{(k)} = [\tilde{x}_1^{(k)}, \tilde{x}_2^{(k)}, \ldots, \tilde{x}_L^{(k)}]^{\mathrm{T}}, \tag{3}$$

where $L = N_{\mathrm{t}}$ and $\tilde{x}_j^{(k)} \in \{0, s_\Re, s_\Im\}$ denotes the transmitted signal in the jth position for the kth user, with $s_\Re$ and $s_\Im$ representing the real and imaginary parts of a QAM symbol s, respectively. Table 1 shows a mapping example for the basic QSM system using 4-QAM and $L = 2$. The first column shows the input bit sequence of length m for the kth user, where the first two bits modulate a 4-QAM symbol and the remaining two bits modulate the indices of non-zero entries in $\tilde{\boldsymbol{x}}^{(k)}$ as follows: the real part of the QAM symbol is assigned to one specific position, whereas the imaginary part can be assigned to another one or even the same position, which are shown in the third column of Table 1. It can be seen from the last column of Table 1 that since $L = 2$, then a total of $2\log_2(L) = 2$ bits can be carried out by the spatial constellation. A detailed review of QSM systems can be found in [6].

2.2 MU interference cancellation

In order to avoid the MU interference, a BD technique is utilised, thus requiring $N_{\mathrm{t}} = KN_{\mathrm{r}}$ in order to have a perfect cancellation of the interference channel matrix. The output vector of the kth QSM block is precoded using the matrix $\boldsymbol{W}_k \in \mathbb{C}^{N_{\mathrm{t}} \times N_{\mathrm{r}}}$. All precoded

signals are then linearly combined to generate the transmission vector $\boldsymbol{x}$ as

$$\boldsymbol{x} = \sum_{i=1}^{K} \boldsymbol{W}_i \tilde{\boldsymbol{x}}^{(i)}. \tag{4}$$

Hence, by substituting (4) into (2), the received signal for the kth user is

$$\boldsymbol{y}_k = \boldsymbol{H}_k \sum_{i=1}^{K} \boldsymbol{W}_i \tilde{\boldsymbol{x}}^{(i)} + \boldsymbol{n}_k, \tag{5}$$

where $\gamma = 1$ is assumed for simplicity. The complete MU–MIMO system in matrix form is expressed as

$$\begin{bmatrix} \boldsymbol{y}_1 \\ \boldsymbol{y}_2 \\ \vdots \\ \boldsymbol{y}_K \end{bmatrix} = \begin{bmatrix} \boldsymbol{H}_1 & \boldsymbol{H}_1 & \cdots & \boldsymbol{H}_1 \\ \boldsymbol{H}_2 & \boldsymbol{H}_2 & \cdots & \boldsymbol{H}_2 \\ \vdots & & \ddots & \vdots \\ \boldsymbol{H}_K & \boldsymbol{H}_K & \cdots & \boldsymbol{H}_K \end{bmatrix} \begin{bmatrix} \boldsymbol{W}_1 \tilde{\boldsymbol{x}}_1 \\ \boldsymbol{W}_2 \tilde{\boldsymbol{x}}_2 \\ \vdots \\ \boldsymbol{W}_K \tilde{\boldsymbol{x}}_K \end{bmatrix} + \begin{bmatrix} \boldsymbol{n}_1 \\ \boldsymbol{n}_2 \\ \vdots \\ \boldsymbol{n}_K \end{bmatrix}, \tag{6}$$

Thus, rearranging the terms, (5) can be rewritten as

$$\boldsymbol{y}_k = \boldsymbol{H}_k \boldsymbol{W}_k \tilde{\boldsymbol{x}}^{(k)} + \boldsymbol{H}_k \sum_{i=1, i \neq k}^{K} \boldsymbol{W}_i \tilde{\boldsymbol{x}}^{(i)} + \boldsymbol{n}_k. \tag{7}$$

The first term in (7) is the signal sent to the kth user whilst the second term is the interference produced by the other users in the system and the third term is the noise. The interference term can be cancelled by the channel if the precoding matrix $\boldsymbol{W}_i$ is designed to satisfy

$$\overline{\boldsymbol{H}}_i \boldsymbol{W}_i = \boldsymbol{0}, \quad i = 1, 2, \ldots, K, \tag{8}$$

where matrix $\overline{\boldsymbol{H}}_i$ contains all system users' matrices except that of the ith user. Thus

$$\overline{\boldsymbol{H}}_i = \left[\boldsymbol{H}_1^{\mathrm{H}}, \ldots, \boldsymbol{H}_{i-1}^{\mathrm{H}}, \boldsymbol{H}_{i+1}^{\mathrm{H}}, \ldots, \boldsymbol{H}_K^{\mathrm{H}}\right]^{\mathrm{H}}. \tag{9}$$

In this manner, (7) is reduced to

$$\boldsymbol{y}_k = \boldsymbol{H}_k \boldsymbol{W}_k \tilde{\boldsymbol{x}}^{(k)} + \boldsymbol{n}_k. \tag{10}$$

For the BD technique, $\boldsymbol{W}_k$ can be obtained decomposing $\overline{\boldsymbol{H}}_i$ into its singular values as

$$\overline{\boldsymbol{H}}_k = \boldsymbol{U}_k [\boldsymbol{\Sigma}_k, \boldsymbol{0}] \left[\boldsymbol{V}_k^{(1)} \boldsymbol{V}_k^{(0)}\right]^{\mathrm{H}}, \tag{11}$$

where $\boldsymbol{U}_k$ is a unitary matrix, $\boldsymbol{\Sigma}_k$ is a diagonal matrix containing the non-negative singular values of $\overline{\boldsymbol{H}}_k$ with dimension equals to the rank of $\overline{\boldsymbol{H}}_k$ and $\boldsymbol{0}$ is an all-zero matrix. $\boldsymbol{V}_k^{(1)}$ contains vectors corresponding to the non-zero singular values and $\boldsymbol{V}_k^{(0)}$ contains vectors corresponding to the zero singular values. The matrix $\boldsymbol{V}_k^{(0)}$ contains the last N_{r} columns of $\boldsymbol{V}_k$, which form an orthogonal basis that is in the null space of $\overline{\boldsymbol{H}}_k$ and can be used as the precoding matrix $\boldsymbol{W}_k$.

Utilising the precoding technique, the MU–MIMO–QSM system can be mathematically modelled as

$$\begin{bmatrix} \boldsymbol{y}_1 \\ \boldsymbol{y}_2 \\ \vdots \\ \boldsymbol{y}_K \end{bmatrix} = \begin{bmatrix} \boldsymbol{H}_1 \boldsymbol{W}_1 & \boldsymbol{0} & \cdots & \boldsymbol{0} \\ \boldsymbol{0} & \boldsymbol{H}_2 \boldsymbol{W}_2 & \cdots & \boldsymbol{0} \\ \vdots & & \ddots & \vdots \\ \boldsymbol{0} & \boldsymbol{0} & \cdots & \boldsymbol{H}_K \boldsymbol{W}_K \end{bmatrix} \begin{bmatrix} \tilde{\boldsymbol{x}}_1 \\ \tilde{\boldsymbol{x}}_2 \\ \vdots \\ \tilde{\boldsymbol{x}}_K \end{bmatrix} + \begin{bmatrix} \boldsymbol{n}_1 \\ \boldsymbol{n}_2 \\ \vdots \\ \boldsymbol{n}_K \end{bmatrix}, \tag{12}$$

2.3 Channel model

In real systems, the channels between different Tx antennas might be correlated. Therefore, the potential multi antenna gains are not always obtained. In order to analyse the spatially correlated MIMO channel, a standard method known as the Kronecker model [19] is considered. Thus

$$\boldsymbol{H}_k^{[\mathrm{corr}]} = \boldsymbol{R}_{\mathrm{r}}^{1/2} \boldsymbol{H}_k^{[w]} \boldsymbol{R}_{\mathrm{t}}^{1/2}, \tag{13}$$

where $\boldsymbol{H}_k^{[\mathrm{corr}]}$ is the matrix of the correlated channel gains between the BS and the ith user. $\boldsymbol{H}_k^{[w]}$ is the flat-fading channel matrix for the kth user, whose elements are assumed to be i.i.d. zero-mean complex Gaussian random variables with unit variance, i.e. $\mathscr{CN}(0, 1)$. Matrices $\boldsymbol{R}_{\mathrm{r}}$ and $\boldsymbol{R}_{\mathrm{t}}$ are the receive and transmit correlation matrices, respectively. The correlation matrices are defined using the exponential model as [20]

$$\boldsymbol{R}_{\mathrm{t}} = \begin{bmatrix} 1 & \rho_{\mathrm{t}} & \rho_{\mathrm{t}}^2 & \cdots & \rho_{\mathrm{t}}^{(N_{\mathrm{t}}-1)} \\ \rho_{\mathrm{t}} & 1 & \rho_{\mathrm{t}} & & \rho_{\mathrm{t}}^{(N_{\mathrm{t}}-2)} \\ \rho_{\mathrm{t}}^2 & \rho_{\mathrm{t}} & 1 & & \vdots \\ \vdots & & & \ddots & \\ \rho_{\mathrm{t}}^{(N_{\mathrm{t}}-1)} & \rho_{\mathrm{t}}^{(N_{\mathrm{t}}-2)} & & & 1 \end{bmatrix} \tag{14}$$

where ρ_{t} is the correlation between adjacent antennas at the transmitter side. A similar matrix $\boldsymbol{R}_{\mathrm{r}}$ with the corresponding correlation coefficient ρ_{r} can be defined in the reception side. The estimated channel $\hat{\boldsymbol{H}}$ in the reception is modelled as [21]

$$\hat{\boldsymbol{H}}_k = \boldsymbol{H}_k^{[\mathrm{corr}]} + \boldsymbol{E}_h, \tag{15}$$

where $\boldsymbol{E}_h \in \mathbb{C}^{N_{\mathrm{r}} \times N_{\mathrm{t}}}$ is the channel estimation error matrix, which is independent of $\boldsymbol{H}_k^{[\mathrm{corr}]}$ and has complex Gaussian elements $\mathscr{CN}(0, \sigma_{\mathrm{e}}^2)$. Therefore, $\hat{\boldsymbol{H}}_k$ has a modified distribution of $\mathscr{CN}(0, 1 + \sigma_{\mathrm{e}}^2)$. In Section 4, (13)–(15) are used to evaluate the performance of the proposed and reference schemes.

2.4 Optimal reception

This subsection discusses the optimal ML detection for the proposed MU–MIMO–QSM scheme. Upon reception, all possible Tx signals are considered to find the most likely one. The optimal ML detector for the proposed scheme is defined as

$$\hat{\tilde{\boldsymbol{x}}}^{(k)} = \arg \min_{j} \| \boldsymbol{y}_k - \hat{\boldsymbol{H}}_k \hat{\boldsymbol{W}}_k \tilde{\boldsymbol{x}}_j \|^2. \tag{16}$$

Let us consider the matrix $\boldsymbol{G}_k = \boldsymbol{H}_k \boldsymbol{W}_k$. Then, a noiseless version of (9) can be written as

$$\boldsymbol{y}_k^{'} = \boldsymbol{G}_k \tilde{\boldsymbol{x}}^{(k)}, \tag{17}$$

where $\boldsymbol{g}_k^{(\ell_{\Re})}$ and $\boldsymbol{g}_k^{(\ell_{\Im})}$ denote the $\ell_{\Re}$th and $\ell_{\Im}$th columns of $\boldsymbol{G}_k$, respectively, with $\ell_{\Re}, \ell_{\Im} \in \{1, 2, \ldots, N_{\mathrm{t}}\}$. Assuming that the CSI is known at the receiver, the optimal ML detector jointly estimates the two active Tx antenna indices, $\hat{\ell}_{\Re}$ and $\hat{\ell}_{\Im}$, as well as the corresponding real-valued signals $\hat{s}_{\Re}^{k}$ and $\hat{s}_{\Im}^{k}$. The vectors $\boldsymbol{s}_{\Re} = \left\{s_{\Re}^{(1)}, \ldots, s_{\Re}^{(q_{\Re})}\right\}$ and $\boldsymbol{s}_{\Im} = j\left\{s_{\Im}^{(1)}, \ldots, s_{\Im}^{(q_{\Im})}\right\}$ represent $q_{\Re}$ and $q_{\Im}$ the real and imaginary parts of all symbols belonging to the M-QAM constellation. The symbol $(\circ)$ represents the Hadamard product among the $\ell_{\Re}$th and $\ell_{\Im}$th columns of $\boldsymbol{G}_k$ and each element of the vectors $\boldsymbol{s}_{\Re}$ and $\boldsymbol{s}_{\Im}$. Then, (15) can be rewritten as

Require: Channel matrix $\mathbf{G}_k$, received vector $\mathbf{y}_k$, $\mathbf{s}_{\Re}$, N_t, N_r
Ensure: The set of tuples ordered $(\hat{\ell}_{\Re}^{(l)}, \hat{s}_{\Re}^{(l)})$
1: Let $\mathbf{d}_1 = [\cdot]$, $\mathbf{tuple}_{\Re} = [\cdot]$
2: **for** $i = 1 : N_t$ **do**
3: Let $\mathbf{d}_1 = \left[\mathbf{d}_1 \quad \| \mathbf{y}_k - \mathbf{g}_k^{(i)} \circ \mathbf{s}_{\Re} \|_F^2\right]$
4: **for** $l = 1 : q_{\Re}$ **do**
5: Let $\mathbf{tuple}_{\Re} = \left[\mathbf{tuple}_{\Re} \quad (\hat{\ell}_{\Re}^{(l)} = i, \hat{\mathbf{s}}_{\Re}^{(l)})\right]$
6: **end for**
7: **end for**
8: Let $[\mathbf{d}_{\Re} \quad \mathbf{ord}_{\Re}] = \mathbf{sort}(\mathbf{d}_1)$ in ascending order.
9: Order $\mathbf{tuple}_{\Re}$ with the same order of $\mathbf{ord}_{\Re}$
10: Return $\mathbf{tuple}_{\Re}$, $[\mathbf{d}_{\Re} \quad \mathbf{ord}_{\Re}]$

Fig. 2 *QSM real part decoding*

Require: Channel matrix $\mathbf{G}_k$, modified received vector $\mathbf{y}_k^{(1)}$, $\mathbf{s}_{\Im}$, N_t, N_r, N_b, V_{th1}
Ensure: The optimum tuple $(\hat{\ell}_{\Im}, \hat{s}_{\Im})$
1: Let $\mathbf{d}_2 = [\cdot]$, $\mathbf{tuple}_{\Im} = [\cdot]$
2: **for** $i = 1 : N_t$ **do**
3: Let $\mathbf{d}_2 = \left[\mathbf{d}_2 \quad \| \mathbf{y}_k^{(1)}(1,1) - \mathbf{g}_k^{(i)}(1,i) \circ \mathbf{s}_{\Im} \|_F^2\right]$
4: **for** $m = 1 : q$ **do**
5: Let $\mathbf{tuple}_{\Im} = \left[\mathbf{tuple}_{\Im} \quad (\ell_{\Im}^{(m)} = i, \mathbf{s}_{\Im}^{(m)})\right]$
6: **end for**
7: **end for**
8: Let $[\mathbf{d}_{\Im} \quad \mathbf{ord}_{\Im}] = \mathbf{sort}(\mathbf{d}_2)$ in ascending order.
9: Order $\mathbf{tuple}_{\Im}$ with the same order of $\mathbf{ord}_{\Im}$
10: Let $lim = N_b$
11: **for** $i = 2 : N_r$ **do**
12: Let $d_{min} = \infty$
13: **for** $m = 1 : lim$ **do**
14: Let $\left(\hat{\ell}_{\Im}^{(m)}, \hat{s}_{\Im}^{(m)}\right) = \mathbf{tuple}_{\Im}(m)$
15: Let $err = \| \mathbf{y}_k^{(1)}(i,1) - \mathbf{g}_k^{(i)}(i, \hat{\ell}_{\Im}^{(m)}) \circ \hat{s}_{\Im}^{(m)} \|_F^2$
16: Let $\mathbf{d}_{\Im}(m) = \mathbf{d}_{\Im}(m) + err$
17: **if** $\mathbf{d}_{\Im}(m) < d_{min}$ **then**
18: Let $d_{min} = \mathbf{d}_{\Im}(m)$
19: Let $\hat{\ell}_{\Im}^{(1)} = \hat{\ell}_{\Im}^{(m)}$ and $\hat{s}_{\Im}^{(1)} = \hat{s}_{\Im}^{(m)}$
20: **else if** $\mathbf{d}_{\Im}(m+1) > V_{th1}$ **then**
21: $lim = m$
22: **break**
23: **end if**
24: **end for**
25: **end for**
26: Return $\left[\hat{\ell}_{\Im}^{(1)}, \hat{s}_{\Im}^{(1)}\right]$,$d_{min}$

Fig. 3 *QSM imaginary part decoding*

$$\left[\hat{\ell}_{\Re}, \hat{\ell}_{\Im}, \hat{s}_{\Re}^{(k)}, \hat{s}_{\Im}^{(k)}\right] = \underset{\ell_{\Re}, \ell_{\Im}, s_{\Re}^{(k)}, s_{\Im}^{(k)}}{\arg\min} \| \boldsymbol{y}_k - \left(\boldsymbol{g}_k^{(\ell_{\Re})} \circ \boldsymbol{s}_{\Re}^{(k)} + \boldsymbol{g}_k^{(\ell_{\Im})} \circ \boldsymbol{s}_{\Im}^{(k)}\right) \|^2, \tag{18}$$

3 Proposed low-complexity detector for the MU–MIMO–QSM scheme

In the previous works [22–26], a number of low-complexity algorithms have been presented for MIMO/SM/QSM signal's detection. In [22, 23], the calculation of optimisation algorithms and trigonometric functions is required in the transmission to estimate the active antennas. As a result, their implementation in practical systems is not easy. On the other hand, in [24–26], algorithms based on tree search and spherical detection demonstrate good BER performance and their detection complexity make them suitable for hardware implementation. In [27], a simple detection algorithm that uses a sub-optimal method based on the least squares solution to detect likely antenna combinations was proposed. Once the antenna indices are detected, ML detection is utilised to identify the transmitted symbols.

In this section, a novel low complexity near ML detector for MU–MIMO–QSM signals is presented. The ML solution to (19) may be expressed as a search tree. Each branch in this tree is assigned a distance metric, where the symbols with the smallest overall distance are selected as the optimum solutions [25, 28]. In our proposal, a novel adaptive *M*-algorithm base on the breadth-first sorted tree search is utilised. The proposed algorithm reduces the search complexity by storing only as maximum the best *M* branches at a time [29]. We define *M* as the maximum number of branches that is necessary to save in order to find the optimal vector. Therefore, a small *M* results in low complexity and relatively sub-optimal performance. As *M* increases, the complexity also increases. However, the performance of the algorithm gets closer to the optimal ML decoder.

The optimisation metrics $\boldsymbol{d}_1$ $\boldsymbol{d}_2$ and d_T required in the near ML detector for the MU–MIMO–QSM scheme can be stated as follows:

$$\boldsymbol{d}_1 = \| \boldsymbol{y}_k - \boldsymbol{g}_k^{(\hat{\ell}_{\Re})} \circ \hat{\boldsymbol{s}}_{\Re}^{(k)} \|_{\mathrm{F}}^2, \tag{19}$$

$$\boldsymbol{d}_2 = \| \boldsymbol{y}_k^{(1)} - \boldsymbol{g}_k^{(\hat{\ell}_{\Im})} \circ \hat{\boldsymbol{s}}_{\Im}^{(k)} \|_{\mathrm{F}}^2, \tag{20}$$

$$d_T = \| \boldsymbol{y}_k - \boldsymbol{g}_k^{(\hat{\ell}_{\Re})} \hat{\boldsymbol{s}}_{\Re}^{(k,l)} - \boldsymbol{g}_k^{(\hat{\ell}_{\Im})} \circ \hat{\boldsymbol{s}}_{\Im}^{(k,m)} \|_{\mathrm{F}}^2. \tag{21}$$

In the proposed algorithm, we denote the *l*th and *m*th symbols in $\boldsymbol{s}_{\Re}$ and $\boldsymbol{s}_{\Im}$ by $\boldsymbol{s}_{\Re}^{(l)}$ and $\boldsymbol{s}_{\Im}^{(m)}$, respectively. The aim of the decoder is to find the optimum solution to the ML criterion in (19), using the distances calculated in (19)–(21). For the case of the distances $\boldsymbol{d}_1$ and $\boldsymbol{d}_2$, they are vectors of distances calculated for each valid combination between each couple of transmitter antennas $\boldsymbol{g}_k^{(\hat{\ell}_{\Re})}$ and $\boldsymbol{g}_k^{(\hat{\ell}_{\Im})}$ to sent the symbols $\boldsymbol{s}_{\Re}$ and $\boldsymbol{s}_{\Im}$, respectively, by the QSM system. The decoding procedure of our algorithm is divided into two parts. First, a pre-ordering based on the vector $\boldsymbol{s}_{\Re}$ is carried out, specifically, the distance of (19) is calculated and symbols are sorted in ascending order. In this way, a set of $N_b = q_{\Re} N_{\mathrm{t}}$ tuples is obtained, each tuple $\left(\hat{\ell}_{\Re}^{(l)}, \hat{s}_{\Re}^{(l)}\right)$ is formed of a combination of the Tx antenna index $\hat{\ell}_{\Re} \in \{1, \ldots, N_{\mathrm{t}}\}$ and the Tx symbol $\hat{\boldsymbol{s}}_{\Re}^{(l)}$. This part of the near ML algorithm is summarised in Algorithm 1 (see Fig. 2).

In the second part, we develop an optimised detector based on the detector proposed for SM signals in [26]. In order to reduce the complexity of the proposed algorithm, two modifications have been made in the search of the optimal vector for the MU–MIMO–QSM transmission system.

In our proposal, the conventional M-algorithm is tailored to the QSM systems to reduce the complexity of the ML detector and to obtain near optimum performance in terms of BER. Since in the first part of the near ML detection algorithm, we estimate the real part of the QSM transmitted symbol $\left(\hat{\ell}_{\Re}^{(l)}, \hat{s}_{\Re}^{(l)}\right)$, in the second part of the near ML detection we consider that only one antenna is active, which corresponds to the imaginary part of the QSM transmitted symbol $\left(\hat{\ell}_{\Im}^{(m)}, \hat{s}_{\Im}^{(m)}\right)$. Therefore, the proposed method performs the search using the following modified received vector

$$\boldsymbol{y}_k^{(1)} = \boldsymbol{y}_k - \boldsymbol{g}_k^{(\hat{\ell}_{\Re}^{(l)})} \circ \boldsymbol{s}_{\Re}^{(l)}, \quad l = 1, \ldots, N_b. \tag{22}$$

The detector performs this operation on each Rx antenna as a level of the tree structure so that the tree search becomes simpler. In each level, a criterion ($V_{\mathrm{th1}} = 2N_{\mathrm{r}}\sigma^2$ and $V_{\mathrm{th2}} = N_{\mathrm{r}}\sigma^2$) based on the metrics of the sphere detector is used to stop the search and discard branches of the tree that are not viable solutions because they exceed the maximum radius of the detection sphere [24, 30]. With this modification, the number of branches for each level is adaptive and depends on the SNR and channel. This part of the near ML algorithm is summarised in Algorithm 2 (see Fig. 3).

Require: Channel matrix $\mathbf{G}_k$,$\mathbf{y}_k$, $\mathbf{s}_{\Re}$, $\mathbf{s}_{\Im}$ N_t, N_r, q, N_b, σ^2, $counter1$, $counter2$

Ensure: Optimum $\left[\hat{\ell}_{\Re}, \hat{s}_{\Re}, \hat{\ell}_{\Im}, \hat{s}_{\Im}\right]$

1: Let $d_T = \infty$, $counter1 = 1$, $counter2 = 1$
2: Let $V_{th1} = 2N_r\sigma^2$ and $V_{th2} = N_r\sigma^2$
3: Execute the *QSM Real part decoding* to obtain $\mathbf{tuple}_{\Re}$, $[\mathbf{d}_{\Re} \quad \mathbf{ord}_{\Re}]$
4: Let $lim = length(\mathbf{tuple}_{\Re})$
5: **for** $m = 1 : lim$ **do**
6: Let $(\hat{\ell}_{\Re}^{(m)}, \hat{s}_{\Re}^{(m)}) = \mathbf{tuple}_{\Re}(m)$
7: Let $\mathbf{y}_k^{(1)} = \mathbf{y}_k - \mathbf{g}_k^{(i)}(i, \hat{\ell}_{\Re}^{(m)}) \circ \hat{s}_{\Re}^{(m)}$
8: Execute the *QSM Imaginary part decoding* to obtain $\left[\hat{\ell}_{\Im}^{(1)}, \hat{s}_{\Im}^{(1)}\right], d_{min}$
9: **if** $d_T < d_{min}$ **then**
10: Let $d_T = d_{min}$
11: Let $\hat{\ell}_{\Re} = \hat{\ell}_{\Re}^{(m)}$
12: Let $\hat{s}_{\Re} = \hat{s}_{\Re}^{(m)}$
13: Let $\hat{\ell}_{\Im} = \ell_{\Im}^{(1)}$
14: Let $\hat{s}_{\Im} = s_{\Im}^{(1)}$
15: **if** $d_{min} < V_{th2}$ **then**
16: $counter1 = counter1 + 1$
17: **if** $counter1 > 2$ **then**
18: **break**
19: **end if**
20: **end if**
21: **else if** $d_{min} > V_{th1}$ and $(V_{th2} < d_T < V_{th1})$ **then**
22: $counter2 = counter2 + 1$
23: **if** $counter2 > 3$ **then**
24: **break**
25: **end if**
26: **end if**
27: **end for**
28: Return $\left[\hat{\ell}_{\Re}, \hat{s}_{\Re}, \hat{\ell}_{\Im}, \hat{s}_{\Im}\right]$

Fig. 4 *Complete near-ML detector*

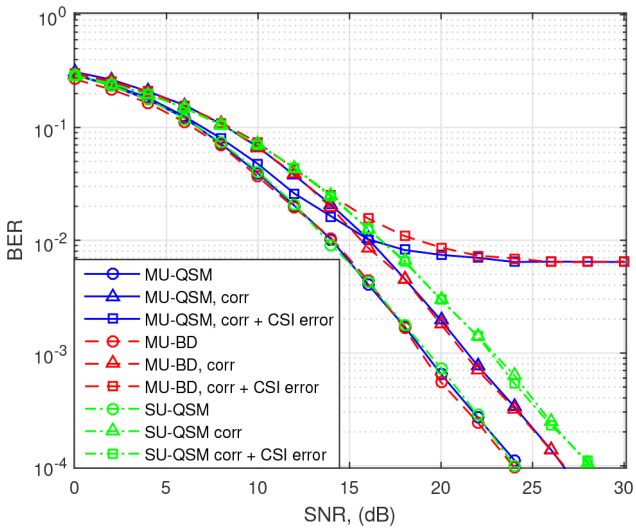

Fig. 5 *Performance comparison for an* $(4 \cdot 2) \times 8$ *configuration at* $m = 4$ *bpcu*

The complete near ML detector is described with details in Algorithm 3 (see Fig. 4). Each iteration produces a symbol estimation $\left[\hat{\ell}_{\Re}, \hat{s}_{\Re}, \hat{\ell}_{\Im}, \hat{s}_{\Im}\right]$ with distance $d_{\min}$. Symbol pairs $\left[\boldsymbol{tuple}_{\Re}, \hat{\ell}_{\Im}, \hat{s}_{\Im}\right]$ whose distances $d_{\min}$ are not smaller than the previous ones are skipped, as specified in line 14. Furthermore, the search is stopped early if the condition in lines 16 and 22 is satisfied. These are the reasons why the proposed algorithm has a significantly reduced complexity.

It is also worth noting that in the proposed algorithm, it is possible to adjust the complexity/BER performance trade-off of the detector by fixing the maximum limit of the variables $counter1$ and $counter2$.

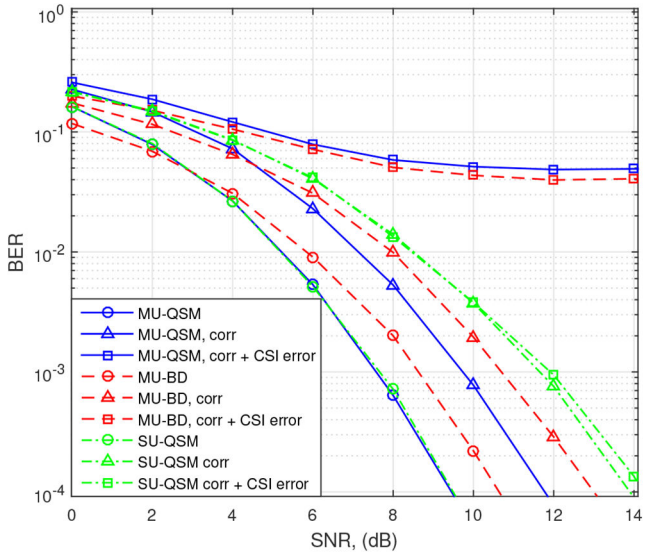

Fig. 6 *Performance comparison for a* $(4 \cdot 8) \times 32$ *configuration and* $m = 8$ *bpcu*

The advantages of our proposal with respect to other similar schemes recently proposed are: compared with [25] our proposal do not require to calculate the QR decomposition; therefore, it is less complex. Compared with [30] our proposal does not require to use complex operations; therefore, it is more suitable for hardware implementation. Also, our proposal is robust to errors in channel estimation and spatial correlation in terms of detection complexity and BER performance.

4 Results

In this section, BER performance results and detection complexity of the proposed scheme are compared to the conventional MU–MIMO–BD scheme for the optimal ML detection algorithm. Furthermore, the BER performance and complexity of the proposed low-complexity detection algorithm are analysed, finally, a simple zero-padding technique is proposed in order to transmit different quantity of bits per channel use to each user in the system.

4.1 BER performance comparison of the MU–MIMO–QSM and the conventional MU–MIMO–BD schemes

In this subsection, two different configurations are used in order to compare the BER performance of the proposed MU–MIMO–QSM scheme with the conventional MU–MIMO–BD scheme for the optimal ML detection under uncorrelated Rayleigh fading channels and correlated fading channels with CSI errors. The simulation parameters used are as follows:

(a) The systems are analysed considering the same SE, and the same number of Tx and Rx antennas.
(b) All systems are using a normalised transmission power of $E[\boldsymbol{x}^{\mathrm{H}}\boldsymbol{x}] = K$.
(c) The correlation coefficients at the transmitter (ρ_{t}) and receiver (ρ_{r}) parts are $\rho_{\mathrm{t}} = \rho_{\mathrm{r}} = 0.7$.
(d) A channel estimation error with $\sigma_{\mathrm{e}} = 0.3\%$ of the Tx power is considered.
(e) For all computer simulations, we target a BER of 10^{-4}.

A BER performance comparison for a $(4 \cdot 2) \times 8$ configuration is shown in Fig. 5. Both the proposed and conventional schemes are using 4-QAM modulation to get a transmission of 4 bpcu for each user. Fig. 6 shows a BER performance comparison for a $(4 \cdot 8) \times 32$ configuration. The MU–MIMO–QSM scheme uses 4-QAM modulation whilst the conventional MU–MIMO–BD scheme uses binary phase shift keying to achieve the transmission of 8

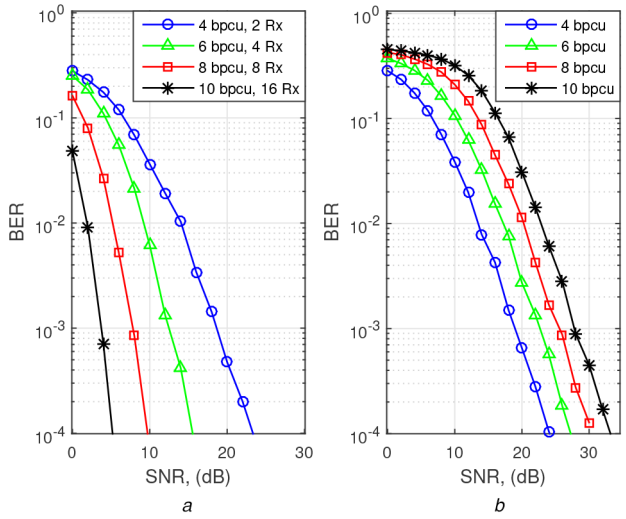

Fig. 7 *MU–MIMO–QSM performance evaluation for variable bpcu per user*

(a) 30 Tx antennas and a variable number of Rx antennas, ***(b)*** 22 Tx antennas and two Rx antennas

Table 2 Comparison of complexity η for the optimal ML detector

Scheme / η	MU–MIMO–BD	MU–MIMO–QSM
$(4 \cdot 2) \times 8$	992	672
$m = 4$	(100%)	(68%)
$(4 \cdot 8) \times 32$	153,600	43,008
$m = 8$	(100%)	(28%)
$(8 \cdot 12) \times 96$	5,117,952	749,568
$m = 12$	(100%)	(7%)

bpcu per user. The same correlation coefficients ρ and the same channel estimation error σ_e are considered. In both graphics, MIMO–QSM for single user (SU) systems is plotted as a reference.

The results of Figs. 5 and 6 show that for the $(4 \cdot 2) \times 8$ configuration both schemes have the same performance for all channel scenarios. However, for the $(4 \cdot 8) \times 32$ configuration, the proposed scheme has 1 dB gain compared with the conventional scheme for both correlated and uncorrelated channels. For both schemes, the considered correlation factor degrades the BER by 2 dB, however, it is observed that small errors in CSI estimation can severely affect the performance of all configurations. This degradation in the performance is more noticeable in configurations with a higher number of antennas, mainly due to the effect on the used precoding matrices where an error in the CSI is introduced. Figs. 5 and 6 also show that the proposed MU–MIMO–QSM method attains the same BER performance of the MIMO–QSM–SU scheme when a perfect CSI is considered. Hence, the utilised precoding technique in the transmission/reception model is effective to cancel the MU interference. However, for correlated channels, the MU schemes show two dBs gain when compared with the MIMO–QSM–SU scheme. This is because, before the transmission in the MU system, the information is dispersed in all Tx antennas, which implies a diversity gain. If a channel with CSI error is considered, MU–MIMO schemes are severely affected in contrast to the MIMO–SU scheme. This can be attributed to the fact that in the MU–MIMO case, a higher number of Tx antennas are used and precoding matrices are also calculated using a channel with errors.

4.2 BER performance of the proposed system for a reduced number of tx/Rx antennas

The conventional MU–MIMO–BD scheme typically uses $N_t = KN_r$ in order to have perfect interference matrix cancellation in the reception [18]. However, this can be a liming factor for practical implementations. In this subsection, two variations to the conventional MU–MIMO–BD scheme are used to shows some flexibility in the proposed MU–MIMO–QSM system. In the first case, different users achieve different SE, i.e. four users receiving 4, 6, 8 and 10 bpcu are considered in the system. In the second case, the users are using different SE and also they are using a reduced number of Rx antennas.

Fig. 7*a* shows the performance for $N_t = 30$ and a variable number of Rx antennas. In order to achieve full precoding cancellation, the total number of Tx antennas N_t is equal to the total number of receive antennas N_r, i.e.

$$N_t = \sum_{i=1}^{K} N_r^{(i)}. \tag{23}$$

Note that in this case, a significant diversity gain is obtained for the users with a higher number of Rx antennas.

In some cases, e.g. if the receivers have space limitations, it can be desirable to use a reduced number of Rx antennas for all users, and at the same time, to receive with different SE at each user. In this case, (23) is not met and the BD technique cannot be used directly. Then, in order to adjust the size of the matrices in the system, we propose to use zero padding. The auxiliary zero-padded matrix $\boldsymbol{H}_{aux}$ for the kth user is defined as

$$\boldsymbol{H}_{k,\text{aux}} = [\boldsymbol{H}_k; zeros(L' - N_r, N_t)] \tag{24}$$

where L' is the virtual size of the transmission vector, which can be used to fix the number of bpcu desired for each specific user. In this way, an appropriate precoding matrix of size $N_t \times L'$ is generated for each user.

Fig. 7*b* shows the performance for users with different SE, $N_t = 22$ and $N_r = 2$. Fig. 7*b* shows that the same SE can be achieved using a reduced number of Tx/Rx antennas with the price of a considerable performance degradation.

4.3 Complexity analysis

The receiver complexities η for the proposed and conventional schemes are evaluated in terms of flops considering the ML detection in (14). A flop is defined as real floating operations, i.e. real additions, multiplications, divisions, and so on. One complex addition and multiplication elaborate two and six flops, respectively [31].

For the conventional MU–MIMO–BD scheme, the lattice in the reception for the case of a SU is composed as

$$\boldsymbol{D}_i = \boldsymbol{H}_i \boldsymbol{W}_i \boldsymbol{B}, \tag{25}$$

where $\boldsymbol{H}_i \in \mathbb{C}^{N_r \times N_t}$, and $\boldsymbol{W}_i \in \mathbb{C}^{N_t \times N_r}$. Multiplication of $\boldsymbol{H}_i \boldsymbol{W}_i$ requires $8N_tN_r^2$ flops and generates a square matrix of dimension $N_r \times N_r$. This matrix multiplies matrix $\boldsymbol{B} \in \mathbb{C}^{N_r \times 2^m}$ and requires $8N_r^2(2^m)$ flops. Each point in matrix $\mathbf{B}$ is an M-QAM signal. Then, generating matrix $\mathbf{D}_i$ requires $8N_r^2(N_t + 2^m)$ flops. Each row in this matrix is used for a different Rx antenna.

Subtractions use $2(2^m)N_r$ flops. Obtaining the magnitude requires $3(2^m)N_r$ flops. Combining all results in a maximum ratio combiner requires $2(N_r - 1)2^m$ flops and finding the minimum requires $2(2^m)$ flops.

Adding all these results, the complexity of the MU–MIMO–BD–ML scheme is

$$\eta_{\text{MU-BD,ML}} \simeq 8N_r^2(N_t + 2^m) + 7N_r(2^m). \tag{26}$$

The complexity of the proposed scheme can be obtained in a similar way. However, in this case, matrix $\boldsymbol{B}$ is a sparse matrix composed of rows where at most two values are different from zero. These values are the real or imaginary parts of the transmitted

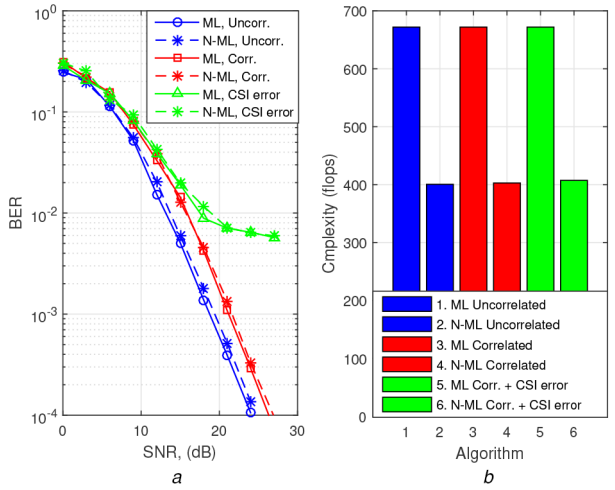

Fig. 8 *Performance comparison of the proposed near-ML algorithm for the MU–MIMO QSM scheme with* $(4 \cdot 2) \times 8$ *configuration*
(a) BER performance, ***(b)*** Detection complexity

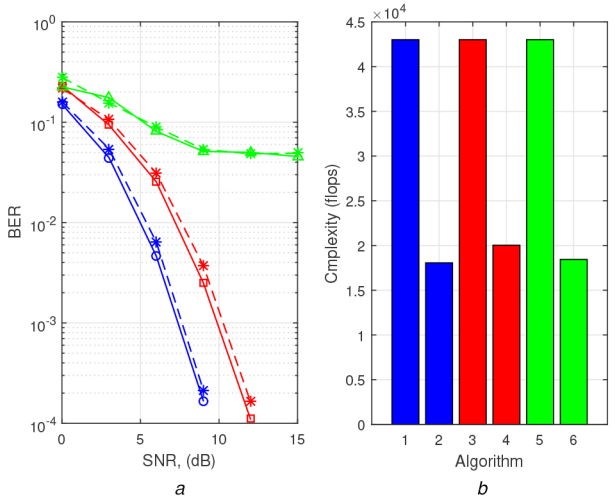

Fig. 9 *Performance comparison of the proposed near ML algorithm for the MU–MIMO–QSM scheme with* $(4 \cdot 8) \times 32$ *configuration*
(a) BER performance, ***(b)*** Detection complexity

QAM symbol. Then, in this case, a reduced complexity can be expected.

For the MU–MIMO–QSM scheme, multiplication by matrix $\boldsymbol{B}$ requires $6(2^m)N_r$ flops. Then, generating matrix $\boldsymbol{D}_i$ requires $8N_tN_r^2 + 6N_r(2^m)$ flops. The rest of the operations are similar to those used for MU–MIMO–BD–ML. Then, by adding the rest of these, the total complexity of the proposed MU–MIMO–QSM–ML detector is

$$\eta_{\mathrm{MU-QSM,ML}} \simeq 8N_tN_r^2 + 13N_r(2^m)\,. \tag{27}$$

Table 2 shows a comparison of complexity per user for the considered two cases and the $(8 \cdot 12) \times 96$ configuration. The complexity of the conventional MU–MIMO–BD scheme is considered as a reference with a complexity of 100%.

For the analysed cases and considering the optimal ML detector, the MU–MIMO–QSM scheme shows a complexity reduction of up to 93% compared with the conventional system.

4.4 Performance of the proposed low-complexity algorithm

In this subsection, the BER performance and complexity of the proposed low complexity detection algorithm for the MU–MIMO–QSM scheme are compared with the conventional MU–MIMO–BD scheme for the $(4 \cdot 2) \times 8$ and the $(4 \cdot 8) \times 32$ configurations and the three types of channels in consideration.

Fig. 8 shows the BER performance comparison for the optimal ML and proposed low complexity near ML algorithms for the MU–MIMO–QSM scheme using the $(4 \cdot 2) \times 8$ configuration and the three channel scenarios; the uncorrelated, the correlated channel, and the correlated channel plus CSI errors. Fig. 8*a* shows the BER performance comparison for the three analysed channel scenarios. Fig. 8*b* shows the detection complexity for the same scenarios. Results show that the proposed near ML algorithm performs very near to the optimal one with the advantage of a reduction in detection complexity of 43%.

The complexity of the ML detector was determined by using (27) defined in Section 4.3. For the near ML detector, the number of flops is evaluated for each symbol transmitted according to the operations required to demodulate a QSM symbol [8], in this evaluation, we include the operations required to carry out the perfect cancellation of the interference matrix in the received signal as defined in Section 4.3. First, the total amount of flops considering all transmitted symbols for a given SNR is considered. Then, this value is averaged between the total number of symbols transmitted for each point of the SNR graph.

Fig. 9 shows the same comparisons as Fig. 8 but for an increased SE of $m = 8$ bpcu per user using a $(4 \cdot 8) \times 32$ configuration. Fig. 9*a* shows the BER performance comparison for the three analysed channel scenarios. Fig. 9*b* shows the detection complexity for the same scenarios. Results show that the BER performance of the proposed algorithm is very close to the optimal ML whilst achieving a reduction in complexity of 58, 53, and 57% for the uncorrelated channel, the correlated channel, and the correlated channel plus CSI errors, respectively.

Note that the proposed low complexity algorithm performs slightly better in the channel with correlation plus CSI errors than in the correlated channel without CSI errors, this is because the similarity in correlated channels makes the decision difficult in the detector. Also, although the proposed algorithm achieves an efficient reduction of complexity in the search three, the initial multiplication intended for MU interference cancellation, achieves almost 70% of the total complexity in the algorithm. This fact makes it difficult for an even higher reduction in complexity.

5 Conclusion

A novel MU–MIMO–QSM downlink transmission scheme which uses the index position in its transmission vector to modulate an independent sequence of input bits for each user in the system has been presented. Additionally, a low-complexity near-ML algorithm for the detection of the MU–MIMO–QSM signal has been proposed. Three different scenarios have been considered: (i) uncorrelated fading, (ii) correlated fading, and (iii) correlated fading with CSI errors. The MU–MIMO–QSM scheme has been compared with the conventional MU–MIMO–BD scheme in terms of the SNR to reach a target BER performance and detection complexity considering the same SE and the same number of Tx and Rx antennas. Results have shown that the proposed scheme outperforms the conventional MU–MIMO–BD in terms of BER by 1 dB. Moreover, the detection complexity of the proposed scheme is up to 93% lower than the reference scheme for the analysed cases. Simulations results also have shown that the MU interference is effectively removed of the system by the utilised technique for the case of an uncorrelated fading channel with perfect CSI. Whilst the spatial correlation slightly affects the BER performance of the simulated MU–MIMO systems, the channel with imperfect CSI significantly degrades the system performance. The proposed low-complexity algorithm performs very near to the optimal ML criterion whilst achieving a complexity reduction of up to 58%.

6 Acknowledgments

The work of E. Basar was supported by the Scientific and Technological Research Council of Turkey (TUBITAK) under Grant 218E035. The work of Francisco R. Castillo-Soria was supported by UASLP under Grant FAI 2019-2020.

7 References

[1] Araújo, D.C., Maksymyuk, T., de Almeida, A.L.F., *et al.*: 'Massive MIMO: survey and future research topics', *IET Commun.*, 2016, **10**, (15), pp. 1938–1946

[2] Wang, C.X., Haider, F., Gao, X., *et al.*: 'Cellular architecture and key technologies for 5G wireless communication networks', *IEEE Commun. Mag.*, 2014, **52**, (2), pp. 122–130

[3] Basar, E., Wen, M., Mesleh, R., *et al.*: 'Index modulation techniques for next-generation wireless networks', *IEEE Access*, 2017, **5**, pp. 16693–16746

[4] Bai, Z., Peng, S., Zhang, Q., *et al.*: 'OCC-selection-based high-efficient UWB spatial modulation system over a multipath fading channel', *IEEE Syst. J.*, 2019, **13**, (2), pp.1181–1189

[5] Wen, M., Zheng, B., Kim, K.J., *et al.*: 'A survey on spatial modulation in emerging wireless systems: research progresses and applications', *IEEE J. Sel. Areas Commun.*, 2019, **37**, (9), pp. 1949–1972

[6] Mesleh, R., Ikki, S.S., Aggoune, H.M.: 'Quadrature spatial modulation', *IEEE Trans. Veh. Technol.*, 2015, **64**, (6), pp. 2738–2742

[7] Mohaisen, M.: 'Increasing the minimum Euclidean distance of the complex quadrature spatial modulation', *IET Commun.*, 2018, **12**, (7), pp. 854–860

[8] Castillo-Soria, F.R., Cortez, J., Gutiérrez, C.A., *et al.*: 'Extended quadrature spatial modulation for MIMO wireless communications', *Phys. Commun.*, 2019, **32**, pp. 88–95

[9] Narasimhan, T.L., Raviteja, P., Chockalingam, A.: 'Generalized spatial modulation in large-scale multiuser MIMO systems', *IEEE Trans. Wirel. Commun.*, 2015, **14**, (7), pp. 3764–3779

[10] Narayanan, S., Chaudhry, M.J., Stavridis, A., *et al.*: 'Multi-user spatial modulation MIMO'. 2014 IEEE Wireless Communications and Networking Conf. (WCNC), Istanbul, Turkey, April 2014, pp. 671–676

[11] Mehana, A.H.: 'Performance of partial block diagonalisation and conjugate beamforming in downlink multiuser MIMO system', *IET Commun.*, 2017, **11**, (10), pp. 1610–1618

[12] Castillo-Soria, F.R., Sanchez-Garcia, J., Maciel-Barboza, M., *et al.*: 'Multiuser MIMO downlink transmission using block diagonalization and generalized spatial modulation techniques', *AEU – Int. J. Electron. Commun.*, 2016, **70**, (9), pp. 1228–1234

[13] Castillo-Soria, F.R., Sánchez-García, J., Parra-Michel, R.: 'Multiuser MIMO downlink transmission using SSK and orthogonal Walsh codes', *Wirel. Pers Commun.*, 2016, **89**, (4), pp. 1089–1102

[14] Humadi, K.M., Sulyman, A.I., Alsanie, A.: 'Spatial modulation concept for massive multiuser MIMO systems', *Int. J. Antennas Propag.*, 2014, **2014**, pp. 1–9

[15] Chen, Y., Wang, L., Zhao, Z., *et al.*: 'Secure multiuser MIMO downlink transmission via precoding-aided spatial modulation', *IEEE Commun. Lett.*, 2016, **20**, (6), pp. 1116–1119

[16] Zhang, M., Miao, W., Shen, Y., *et al.*: 'Joint spatial modulation and beamforming based on statistical channel state information for hybrid massive MIMO communication systems', *IET Commun.*, 2019, **13**, (10), pp. 1458–1464

[17] Siregar, R.F., Rajatheva, N., Latva-aho, M: 'QSM based NOMA for multi-user wireless communication'. 2019 16th Int. Symp. on Wireless Communication Systems (ISWCS), Oulu, Finland, August 2019, pp. 139–144

[18] Spencer, Q.H., Swindlehurst, A.L., Haardt, M.: 'Zero-forcing methods for downlink spatial multiplexing in multiuser MIMO channels', *IEEE Trans. Signal Process.*, 2004, **52**, (2), pp. 461–471

[19] Yu, K., Bengtsson, M., Ottersten, B., *et al.*: 'A wideband statistical model for NLOS indoor MIMO channels'. Proc. IEEE 55th Vehicular Technology Conf., Birmingham, AL, USA, May 2002, vol. 1, pp. 370–374

[20] Paulraj, A., Nabar, R., Gore, D.: '*Introduction to space-time wireless communications*' (Cambridge University Press, Cambridge, UK, 2003)

[21] Basar, E., Aygolu, U., Panayirci, E., *et al.*: 'Performance of spatial modulation in the presence of channel estimation errors', *IEEE Commun. Lett.*, 2012, **16**, (2), pp. 176–179

[22] Li, J., Jiang, X., Yan, Y., *et al.*: 'Low complexity detection for quadrature spatial modulation systems', *Wirel. Pers. Commun.*, 2017, **95**, (4), pp. 4171–4183

[23] Yigit, Z., Basar, E.: 'Low-complexity detection of quadrature spatial modulation', *Electron. Lett.*, 2016, **52**, (20), pp. 1729–1731

[24] Al-Nahhal, I., Dobre, O.A., Ikki, S.S.: 'Quadrature spatial modulation decoding complexity: study and reduction', *IEEE Wirel. Commun. Lett.*, 2017, **6**, (3), pp. 378–381

[25] Jiang, Y., Lan, Y., He, S., *et al.*: 'Improved low-complexity sphere decoding for generalized spatial modulation', *IEEE Commun. Lett.*, 2018, **22**, (6), pp. 1164–1167

[26] Zheng, J., Yang, X., Li, Z.: 'Low-complexity detection method for spatial modulation based on M-algorithm', *Electron. Lett.*, 2014, **50**, (21), pp. 1552–1554

[27] Altin, G., Celebi, M.E.: 'A simple low complexity algorithm for generalized spatial modulation', *AEU – Int. J. Electron. Commun.*, 2018, **97**, pp. 63–67

[28] Anderson, J., Mohan, S.: 'Sequential coding algorithms: a survey and cost analysis', *IEEE Trans. Commun.*, 1984, **32**, (2), pp. 169–176

[29] Hassibi, B., Vikalo, H.: 'On the sphere-decoding algorithm: I. Expected complexity', *IEEE Trans. Signal Process.*, 2005, **53**, (8), pp. 2806–2816

[30] Xiao, L., Yang, P., Xiao, Y., *et al.*: 'Efficient compressed sensing detectors for generalized spatial modulation systems', *IEEE Trans. Veh. Technol.*, 2017, **66**, (2), pp. 1284–1298

[31] Khan, M.H.A., Cho, K.M., Lee, M.H., *et al.*: 'A simple block diagonal precoding for multi-user MIMO broadcast channels', *EURASIP J. Wirel. Commun. Netw.*, 2014, **2014**, (1), pp. 1–8